

Chitosan-Sodium Alginate Polyelectrolyte Complex Coating Pluronic® F127 Nanoparticles Loaded with Citronella Essential Oil

Mariele P. Sanches,^a Idejan P. Gross,^a Rodrigo H. Saatkamp,^a Alexandre L. Parize^a and Valdir Soldi^{✉*,a,b}

^aGrupo de Estudo em Materiais Poliméricos (Polimat), Departamento de Química, Universidade Federal de Santa Catarina, 88040-900 Florianópolis-SC, Brazil

^bInstituto Brasileiro de Tecnologia do Couro, Calçado e Artefatos (IBTeC), 93334-000 Novo Hamburgo-RS, Brazil

Pluronic® F127 nanoparticles were loaded with citronella essential oil (CEO) and then covered with chitosan-sodium alginate polyelectrolyte complex (PEC). The system was characterized according to size, zeta potential and stability over time. Dynamic light scattering (DLS) in different proportions of water/ethanol as a dispersive medium was important in confirming that PEC covered the F127 nanoparticles. Infrared spectroscopy also indicated interaction of F127 with PEC. The nanoparticle size evaluated by transmission electron microscopy (TEM) and field emission scanning electron microscopy (FESEM) corroborated the value observed in DLS (hydrodynamic radius (R_H) range of 100-200 nm). Encapsulation efficiency of 80% for CEO was determined by UV-Vis spectroscopy. The release profile of the CEO was evaluated in phosphate buffer saline (PBS) containing 20% of ethanol and in simulated sweat fluid, achieving 74 and 81%, respectively. The releasing mechanism fitted the Korsmeyer-Peppas mathematical model, indicating Fickian diffusion behavior for both studied media.

Keywords: citronella essential oil, encapsulation efficiency, nanoparticles, polyelectrolyte complex

Introduction

Essential oils are volatile compounds, constituted by polyunsaturated fatty acids, polyphenols, tocopherols, monoterpenes, flavonoids, carotenoids, steroids and xanthophylls. Therefore, they present many biological activities, allowing application in pharmaceuticals,¹ cosmetics,² food conservation,³ and textile technologies⁴ to explore properties such as antifungal, bactericidal and insect repellence.⁵ The majority compounds of citronella essential oil (CEO) are the monoterpenes citronellal, geraniol and citronellol, which are responsible for attaching to the insect's odor receptor protein and masking the host's odor, conferring repellence activity. Some studies have also reported the fungicidal property of citronella oil in function of citronellal, α - and β -pinenes.⁶ However, essential oils exhibit a high rate of evaporation of volatile molecules due to high vapor pressure. So, encapsulating these active compounds is a viable alternative to preserve

and improve their chemical and biological properties.⁷ For this purpose, the use of carrier systems shaped as micelles and nanoparticles is a promising alternative.

The use of biopolymers such as the polysaccharides chitosan and sodium alginate to encapsulate essential oils⁸ has been much studied due to their properties such as biocompatibility, non-toxicity and biodegradability, besides the wide availability of raw materials. Chitosan is derived from chitin deacetylation and comprises two monomeric units: β -D-glucosamine and *N*-acetyl glucosamine.⁹ Sodium alginate consists of a linear chain that has a unit of β -D mannuronic acid (M) linked to α -L-guluronic acid (G).¹⁰ Polysaccharides are presented in their ionic form in a solution whose pH covers their pK_a range.¹¹ In this ionic form, polysaccharides assume a polyelectrolyte behavior, making aggregation in nanoparticles possible via electrostatic interaction, creating a polyelectrolyte complex (PEC).¹² A chitosan solution whose pH has to be lower than 6.5, to avoid gelation or precipitation, and a sodium alginate solution whose pH is higher than 3.6 are required to form a PEC, by the presence of positive charges in chitosan and negative

*e-mail: soldi.valdir@gmail.com

charges in sodium alginate, resulting in a structure that is mechanically stronger if compared to isolated polymers.

Nevertheless, knowing the hydrophobic nature of essential oils,¹³ it makes the use of a surfactant indispensable to their encapsulation with hydrophilic polymers. Pluronic® F127 is an amphiphilic block copolymer constituted by hydrophilic poly(oxyethylene) and hydrophobic poly(oxypropylene) blocks (PEO₉₈-PPO₆₇-PEO₉₈),¹⁴ which have been used to stabilize this kind of compound in a hydrophilic environment, by reducing vapor pressure and, consequently, volatilization.¹⁵

In this context, the purpose of this work was to prepare and characterize nanoparticles from Pluronic® F127 covered with chitosan/sodium alginate complex. The release profile of citronella essential oil incorporated in the nanoparticles and the system stability were also evaluated.

Experimental

Materials

The polymeric nanoparticles were prepared using medium molar mass chitosan (87% degree of deacetylation), viscosimetric molar mass (M_v) = 10.6×10^4 g mol⁻¹; sodium alginate, M_v = 31.1×10^4 g mol⁻¹; and block copolymer Pluronic® F127, all purchased from Sigma-Aldrich® (St. Louis, USA). Citronella (*Cymbopogon winterianus*) essential oil was purchased from Harmonia Natural, Canelinha-SC, Brazil.

Citronella essential oil chemical profile

CEO was characterized regarding to chemical compounds by gas chromatograph (GC) Agilent Technologies (GC 7890A, United States) coupled to a mass spectrometer (MS, 5975C) with a capillary column HP-5MS (Agilent Technologies), dimethylsiloxane/phenyl (95:5) as stationary phase and helium as carrier gas (1 mL min⁻¹). The characterization of the essential oil is shown in the Supplementary Information (SI) section.

Oil-loaded nanoparticle preparation

The nanoparticles were prepared in three steps. Firstly, an emulsion of Pluronic® F127 (0.05% m/v) containing 200 µL of CEO was prepared in ethanol under magnetic stirring. Then, 1 mL of this emulsion was dropped in a chitosan solution (0.15% m/v, pH = 4.0) previously prepared in acetic acid 1% (v/v), remaining under magnetic stirring for 30 min. In the third step, the PEC formation occurred by the addition of sodium alginate (0.15% m/v,

pH = 6.0) to chitosan-F127 emulsion in a volumetric ratio of 25:5 (chitosan/sodium alginate) under Ultra Turrax® homogenization (20 min at 5000 rpm).

Ethanol/water composition effect on the hydrodynamic radius of the systems

This study was carried out in order to verify how the polyelectrolyte complex could stabilize the Pluronic® F127 micelles, with an initial hypothesis that it is by covering. The nanostructured systems were prepared according to the procedure described above. F127/citronella oil and F127/citronella oil stabilized with chitosan-alginate PEC were evaluated by ranging the H₂O/ethanol volume ratio of the dispersion medium. After the preparation procedure, 1.0 mL of the nanoparticle suspension was collected and diluted with 9.0 mL of H₂O/ethanol solution at different volume ratios, namely, 100/0, 95/5, 90/10, 85/15, 80/20, 75/25, 70/30, 60/40 and 50/50 for F127/citronella oil and 100/0, 90/10, 80/20, 75/25 PEC. Then, the suspensions were filtered using a 0.45 µm Sartorius® filter membrane and analyzed by dynamic light scattering (DLS) using ALV-LSE 5004 equipment, by taking the correlation curves at 90°. The correlation curves supported the establishment of the hydrodynamic radius (R_H) and, therefore, provided information about the size of the nanoparticles as a function of the ethanol volume fraction. The results are thoroughly discussed in the Results and Discussion section.

Nanoparticle characterization

The determination of hydrodynamic radius and polydispersity index (PDI) was performed in a Multicorrelator Goniometer (ALV-LSE 5004, Germany) with a HeNe linearly polarized laser at the wavelength of 632.8 nm. The scattered light was verified in the range of 30-150°, at intervals of 10° and for each angle analyzed was obtained the relaxation frequency (G). The diffusion coefficient (D) was obtained from the angular coefficient of the relaxation frequency plot as a function of the wave vector, q, according to equation 1:

$$\frac{G}{q^2} = D \quad (1)$$

The wave vector q is defined by equation 2:

$$q = \frac{4\pi n}{\lambda} \sin \frac{\theta}{2} \quad (2)$$

where λ is the wavelength of incident light, θ the scattering

angle and n the refraction index. Knowing the diffusion coefficient (D) (equation 1), from Stokes-Einstein equation (equation 3), in which k_B is the Boltzmann constant, T is the sample temperature and η the medium viscosity, it is possible to calculate the R_H of the nanoparticles.

$$R_H = \frac{k_B T}{6\pi\eta D} \quad (3)$$

To proceed the analysis, 1.0 mL of the nanoparticle suspension was collected and diluted with 9.0 mL of ultrapure water and filtered using a 0.45 μm Sartorius® filter membrane.

The zeta potential was measured using a Malvern Zetasizer (Malvern Instruments, UK) with a wavelength of 633 nm at 25 °C without sample dilution. All measurements were performed in triplicate by means of Helmholtz-Smoluchowski approximation.

Stability control related to the size, zeta potential and pH was monitored utilizing the methodology described above. The measurements were done on freshly prepared nanoparticles, at 7, 14, 28, 45, 60 days and at 1 year after preparation.

The transmission electron microscopy (TEM) images were taken using a JEM-1011 at an accelerating voltage of 80 kV. Suspension of the sample solution was diluted in water/isopropyl alcohol or in water/ethanol, filtered using a 0.45 μm Sartorius® filter membrane and dropped onto a carbon-copper grid, subsequently negatively stained with 1% uranyl acetate. The grid was dried for 24 h before the analysis.

The morphology of the freshly prepared nanoparticles was also evaluated using a JEOL JSM-6701F field emission scanning electron microscopy (FESEM) at an accelerating voltage of 10 kV by dropping the sample without dilution onto a silica plate streaked on an aluminum stub for further gold recovery.

In order to obtain the Fourier transform infrared (FTIR) spectra, the sample including pure chitosan and sodium alginate solution was dried in a Spray Dryer BUCHI B198 (Switzerland), inlet and outlet temperature of 160 and 110 °C, respectively, and flow rate of 2.4 mL min⁻¹. The FTIR spectra of the powders obtained in the Spray Dryer were performed with a Shimadzu Prestige-21 (Japan) with KBr pellets, and the data were collected over the range of 4000–400 cm⁻¹ with resolution of 2.0 cm⁻¹.

Determination of encapsulation efficiency and *in vitro* release study

The encapsulated CEO content was determined by UV-Vis spectrophotometry (UV NOVA/1800, Brazil)

technique. Firstly, the sample was centrifuged utilizing a Viva Spin turbo4, Sartorius, at 7000 rpm for 20 min. The centrifuged content was lysed through acetic acid, then 1 mL of hexane was added with the aim of extracting the oil content. The absorbance was measured at 210 nm. The amount of loaded CEO was calculated by a standard curve, which was prepared with different CEO concentrations in pure hexane at 210 nm. In this way, the encapsulation efficiency (EE) was calculated according to equation 4:

$$EE(\%) = \frac{\text{Total concentration of CEO}}{\text{Initial concentration of CEO}} \times 100 \quad (4)$$

The *in vitro* release study was performed using the dialysis method. For this, a cellulose acetate bag with a cut of 10×10^3 g mol⁻¹ was previously soaked in deionized water to remove the preservatives. Then 30 mL of oil-loaded nanoparticle was placed in the dialysis bag surrounded by 500 mL of dissolution medium at 37 °C. In order to compare the release mechanism, two different media were used, phosphate-buffered saline (PBS) solution at pH 5.5 containing 20% of ethanol to help release the essential oil more uniformly, as previously described in Natrajan *et al.*,¹⁶ and the simulated sweat fluid prepared based on Kulthong *et al.*¹⁷ description. These two releasing processes were conducted over 24 h, and 3 mL of the medium was removed from solution medium in a certain time to be quantified by UV-Vis spectrophotometry (UV NOVA/1800, Brazil). The experiment was done in triplicate for each release medium, and the amount released was calculated according to equation 5 considering sink conditions along the experiment up to the essential oil solubility in the solvents (1.3 $\mu\text{L mL}^{-1}$ solubility in PBS containing 20% of ethanol and 0.9 $\mu\text{L mL}^{-1}$ in sweat fluid).

$$\text{Release}(\%) = \frac{[\text{Released oil}]}{[\text{Total oil}]} \times 100 \quad (5)$$

Results and Discussion

Citronella essential oil chemical profile

The GC-MS analysis was done in order to identify the chemical compounds in citronella oil, comparing the results to spectral data from the NIST11 library, thus evaluating its potential use as an active agent in antifungal applications. Eight compounds were identified: D-limonene, citronellal, citronellol, β -pinene, 3-carene, β -(D)-elemene, D-cadinene, cycloheptane and 4-methylene-1-methyl-2-(2-methyl-1-propen-1-yl)-1-vinyl. Among them, citronellal, β -pinene and citronellol

are the major compounds, representing 63.5, 14.9 and 7.5% of the total CEO constituents, respectively. Further information about the retention time (Table S1) and the corresponding chromatogram (Figure S1) can be found in the SI section. Some of the above identified CEO compounds were characterized as substances with potential antimicrobial activity. For example, Alves-Silva *et al.*¹⁸ reported an antimicrobial effect of β -pinene, one of the major CEO constituents, against the fungus *C. neoformans* by inhibition of the phospholipase and stearase activities. El-Kholany¹⁹ verified a strong antifungal potential against *A. flavus* and *G. candidum*, confirming that the CEO changed the cellular permeability causing leakage of fungal cytoplasm. CEO was also evaluated as having repellence activity against *Aedes aegypti* when encapsulated in gelatin and guar gum microparticles.²⁰

Dynamic light scattering

Figure 1 shows the correlation curves (Figure 1a) and the hydrodynamic radius distribution (Figure 1b), unweighted logarithmic mode, obtained from the nanoparticulate system. A bimodal size distribution can be seen, probably resulting from polymer chain size variation and polyelectrolyte ionization degree. According to ALV-7004 Correlator Software V.3.0,²¹ approximately 18% of the total population has an R_H value of 38 nm and 82% of 196 nm. According to Avadi *et al.*,²² PDI value of 0.39 indicates a homogeneous dispersion, since this system is made of natural polymers, suggesting also that the formation of smaller particles is due to a stronger electrostatic interaction.

In order to evaluate if the copolymer Pluronic® F127 loaded with essential oil nanoparticles were covered by

the PEC chitosan-sodium alginate, DLS measurements were performed to evaluate the effect of ethanol/water composition as dilution medium on the hydrodynamic radius of the systems.

Copolymer samples (0.05%; m/v) prepared in two ways: pure ethanol with or without addition of CEO and pure water with or without addition of CEO, were analyzed by DLS. Those samples that did not contain CEO did not indicate formation of nanostructures, since the correlation function did not fit in exponential form, suggesting that in this condition, F127 unimers remained free in solution.¹⁵ However, for Pluronic® F127 nanoparticles (0.05%; m/v) prepared in ethanol with CEO addition, the obtained correlation curve reveals the formation of nanostructures of 146 nm. According to Ashraf *et al.*,²³ this behavior can be associated with the improvement in the hydrophobicity of the PPO block and the decrease in the hydrophilicity of the PEO block.

All the correlation curves obtained by varying the ethanol volume fraction in the suspension dilution step, as detailed in the Experimental section, are presented in Figures S2a and S2b in the SI section. As can be seen, as the percentage of ethanol increased, the correlation function ($G(\tau)$) shifted to higher decay times, suggesting the formation of elongated nanoparticles. The shape distortion (elongated and not spherical nanoparticles) is related to the longer time during which the particles are submitted to the incident beam from the DLS instrument, due to Brownian motion.²⁴

Figure 2 shows the R_H values as a function of ethanol volume percentage in dispersive medium for Pluronic® F127 prepared in ethanol containing CEO (blue triangle curve) and for the copolymer covered with chitosan and sodium alginate (red circle curve). For Pluronic® F127, the expansion until 30% of ethanol in the medium is

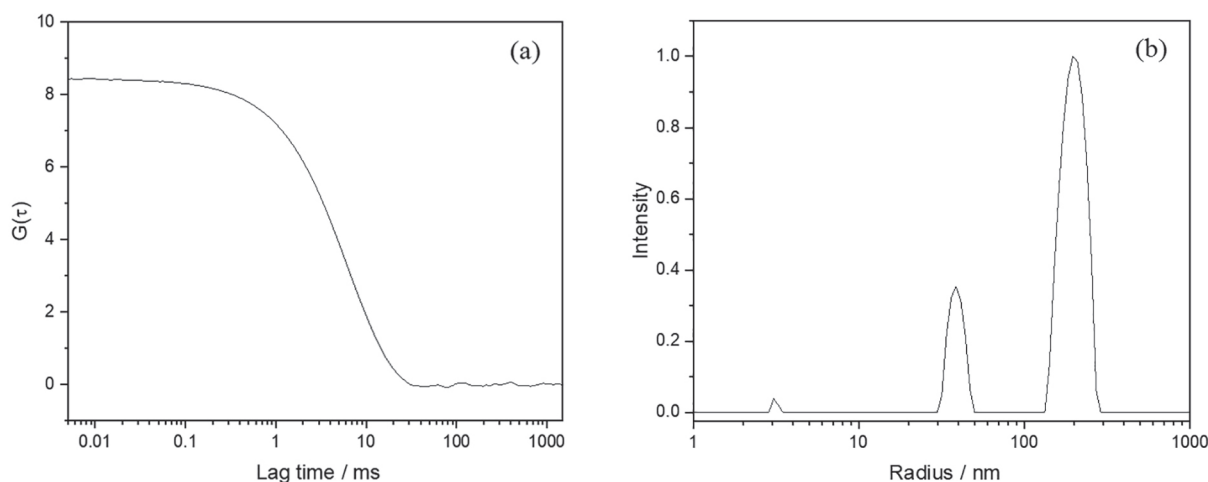


Figure 1. Correlation curves (a) and radius distribution (b) for CEO-loaded PEC.

remarkable, and approximately the same size was observed up to 50%. However, the disruption of nanoparticle structure was observed at about 35% of ethanol, and once above this ethanol content, the intensity of light scattered decreases dramatically. As ethanol is a good solvent for both PPO and PEO blocks, the increase in nanoparticle size is related to the core and shell swelling (block solvation).

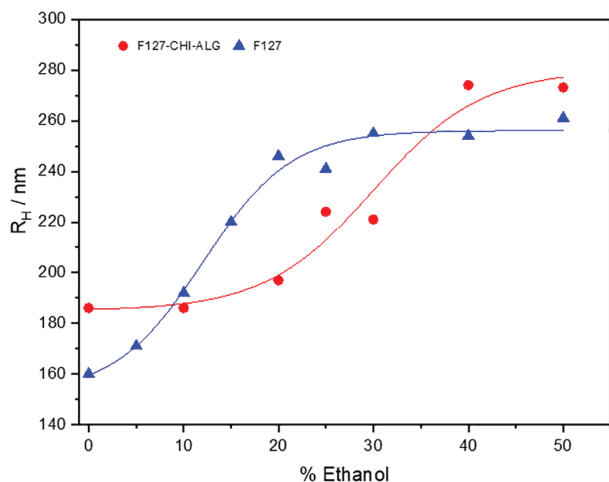


Figure 2. Effect of ethanol percentage on the R_H values of Pluronic® F127 loaded with citronella essential oil and the same system covered with chitosan-sodium alginate (PEC).

In the presence of chitosan and sodium alginate a different R_H profile was observed. The nanoparticles increased in size due to the coating created by the two polymers, which prevents the solvation of Pluronic®. Almost the same R_H value was observed until 20% of ethanol. However, from 25% upwards, the R_H value increased, suggesting that the ethanol molecules entered the polymer chain, inducing nanoparticle disruption and/or aggregation. This can be observed between 30 and 50% of ethanol, where the intensity of scattered light strongly decreased, in step with the decrease in the lag time.

As described in the literature,^{25,26} chitosan interacts with Pluronic mainly by electrostatic effect. The electronegative oxygen of PEO links to electropositive chitosan chains via ion-dipole interaction. Studies performed by Pepic *et al.*²⁵ showed that due to the Pluronic® F127 and chitosan interaction, the hydrodynamic radius of the nanoparticles increased and the zeta potential values decreased. The results were attributed to interaction between the oxygen atoms of the PEO (Pluronic) and the electropositive chitosan. In the present work we are suggesting that chitosan from PEC complex interacts with oxygen of the PEO segment, justifying the particle stabilization through the blockage of ethanol from the dispersive medium to the F127 nanoparticles, explaining why a larger ethanol volume fraction is required to increase the particle size.

Zeta potential

In acid medium, chitosan is a polycation due to ammonium groups formed by amine group protonation on the polymer structure. Therefore, when the polyanion sodium alginate is dropped into a chitosan solution there is an intermolecular electrostatic interaction forming the complex.²⁷ Since the anionic-cationic charge ratio of the molecules is involved in the formation of PEC, the positive zeta potential value obtained, 54.3 mV, indicates an excess of positive charges, and so the nanoparticles are in chitosan solution.

Stability control as a function of storage time

The storage of the nanoparticles over sixty days resulted in an increase of the particle size from 130 to 188 nm and the PDI from 0.39 to 0.50 due to the agglomeration process of the small particles. The zeta potential values had a slight decrease from 54.3 to 44 mV over the same time and, as suggested by Wu *et al.*,²⁸ the electrostatic interactions between the nanoparticle components may be responsible for reduction of the positive charges. On the other hand, the pH values increased from 3.32 to 4.41. This is in accordance with the behavior observed by Furtado *et al.*²⁹ for chitosan/NaF nanoparticles. This behavior is due to the proximity of the pH value to chitosan pK_a , which decreases the dissolution capacity of the polymer, inducing the formation of agglomerates (in the flask). Although the formation of agglomerates and an increase in the particle size and pH were observed, the zeta potential remained above 30 mV, which is considered a value for a physically stable system.

FESEM and TEM of nanoparticles

In accordance with the DLS results, polydisperse nanoparticles with size ranging from 100 to 200 nm were observed by TEM image (Figures 3a-3d). Figures 3a-3b were obtained from isopropyl alcohol/water dilution and Figures 3c-3d from ethanol/water dilution in proportion 20:80 (% v/v). Until this quantity of ethanol, the TEM images (Figures 3c-3d) confirmed the coating process due to the presence of PEC. Also, the nanoparticles size increased about 60 nm in relation to those without ethanol. The DLS correlation suggested the formation of spherical nanoparticles in the presence of encapsulated essential oil in Pluronic F127, whose shape is maintained even after covering with the biopolymers.³⁰ As suggested by Barradas *et al.*,³¹ the system may suffer flattening and also dehydration during the drying process, leading to a

smaller size than that observed in DLS measurements. Tagliari *et al.*,³² in a study of glycyrrhizic acid encapsulation in chitosan and alginate nanoparticles, attributed the observed dense surface to active adsorption. In order to obtain a clearer and more detailed surface image than TEM could provide, FESEM analysis was also carried out, and those images can be seen in Figure 4. Nanoparticles with softened surface and uniform droplet size were observed, due to the different drying process. Obtaining nanostructures with a uniform droplet size becomes essential in achieving a stable system³³ whose observation

is in accordance with nanoparticle stability which, even one year later, remained stable.

FTIR spectroscopy for dried nanoparticles

This analysis was conducted with the aim of evaluating the interaction among the functional groups of the biopolymers with the copolymer block. Pure chitosan and sodium alginate solution prepared at the same pH value were used to produce the nanoparticles and were also dried in the Spray Dryer. The FTIR spectra are shown in Figure 5.

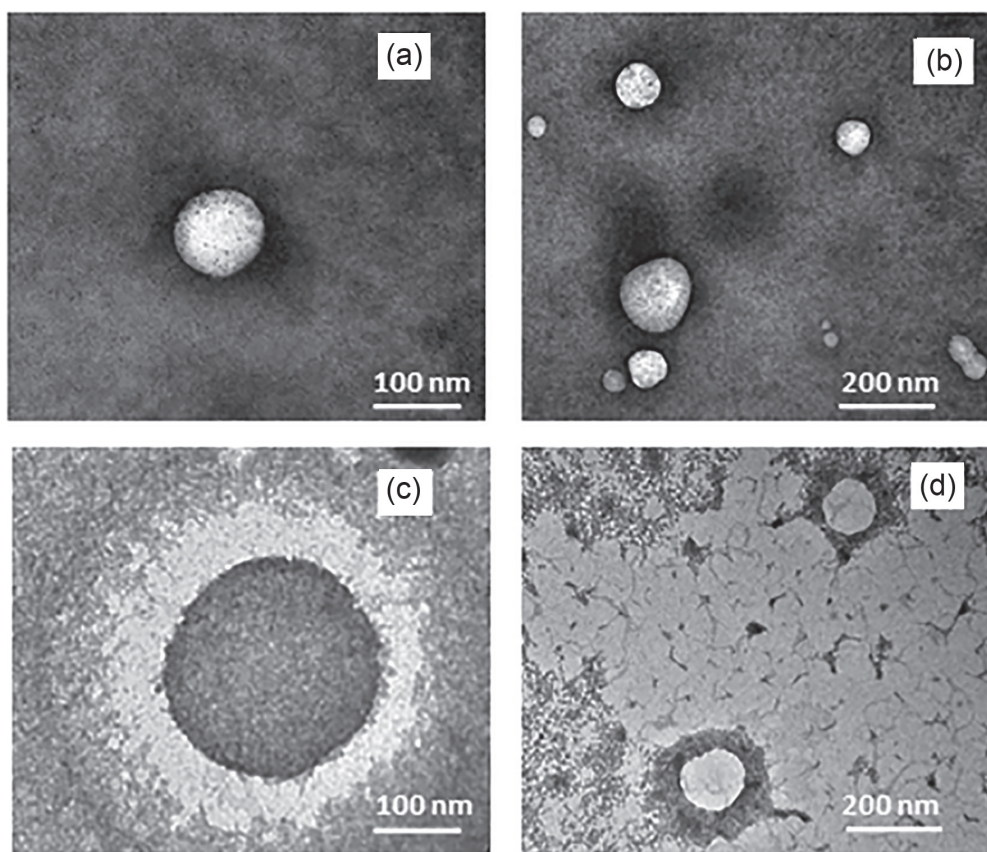


Figure 3. Spherical shape for chitosan/alginate PEC coating Pluronic nanoparticles by TEM microscopy. (a, b) Obtained from isopropyl alcohol/water dilution; (c, d) ethanol/water dilution 20:80 (%v/v).

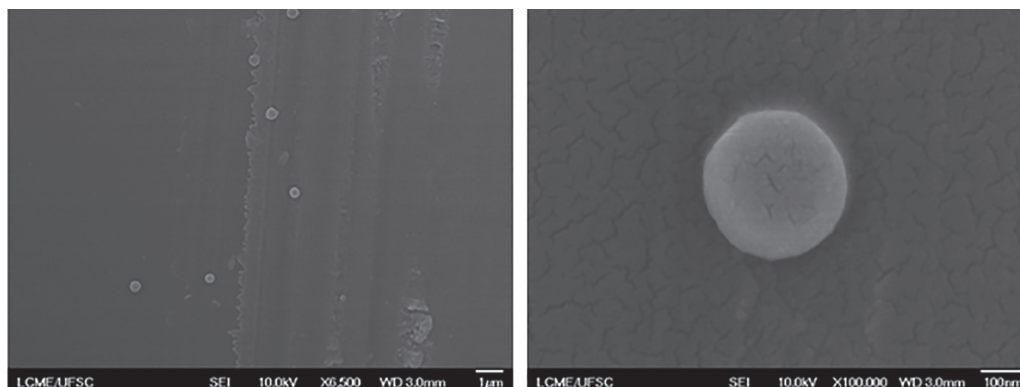


Figure 4. Softened surface observed for loaded chitosan-alginate PEC in FESEM images with magnification of 6,500× (left image) and 100,000× (right image).

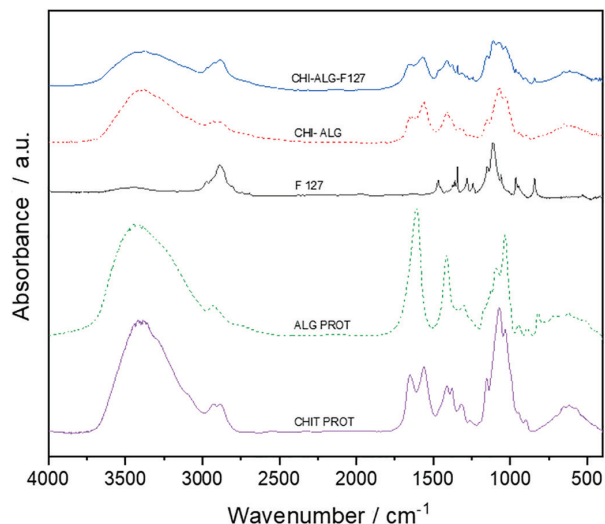


Figure 5. Infrared spectra of chitosan, sodium alginate, F127, chitosan-alginate PEC and F127 nanoparticle.

Some major absorption peaks can briefly identify the polymers. For chitosan (purple line), the broad absorption bands at 3400 cm^{-1} are linked to N–H and O–H stretching vibration. The absorption bands at 1653 , 1564 , 1377 and 1067 cm^{-1} are related to the C=O stretching of the secondary amide, bending vibrations of the *N*-acetylated residues, C–N and C–O–C stretching vibration, respectively. On the green line, for pure sodium alginate, the broad absorptions at 3400 and 2930 cm^{-1} are related to O–H and C–H stretching, respectively. Absorption peaks at 1609 and 1411 cm^{-1} are associated with asymmetric and symmetric CO_2 stretching vibrations, respectively. The peak at 1085 cm^{-1} corresponds to C–O–C asymmetric stretching. On the black line for pure F127, the absorptions at 1341 , 1278 , 1243 and 964 cm^{-1} are related to CH_2 stretching vibration, and C–O–C vibration is observed at 1114 cm^{-1} .

On the red and dark blue lines, the absorption bands at 3340 cm^{-1} are attributed to the hydroxyl and amino groups from alginate and chitosan, respectively. Natrajan *et al.*¹⁶ suggest that these interactions between functional groups induce PEC formation due to the electrostatic interaction between the poly ions. In the alginate spectra, the absorption band at 1609 cm^{-1} shifted to 1650 cm^{-1} suggesting interaction of the carboxylate group with chitosan. The absorption band on the chitosan-alginate (PEC), green line, observed at 1560 cm^{-1} , represents the stretching of NH_2 groups from chitosan. The main absorption bands present in the Pluronic[®] spectra are also observed in the nanoparticle formed with F127 and PEC. On the dark blue line, a shift of the band at 1560 to 1568 cm^{-1} was observed, indicating hydrogen bonding interaction between PEC and the O–H terminal group of F127.

FTIR spectroscopy analysis was also used to determine the chitosan deacetylation degree (CDD, in percentage) and the ratio between mannuronic and guluronic acids (M/G) in sodium alginate. The CDD gives information about the reticulation capacity of anionic species, solubility and chain conformation. Considering the Brugnerotto *et al.*³⁴ methodology, a deacetylation degree of 87% was obtained. The ratio (M/G) in sodium alginate determined by the methodology proposed by Filippov and Kohn³⁵ was 1.03 (50.7% of M and 49.3% of G). To prepare nanoparticles by ionic gelation it is important to use a polymer containing a high guluronic acid content, since this polysaccharide proportion will interact with other polymers by electrostatic interaction.³⁶

Encapsulation efficiency and *in vitro* release for citronella essential oil

The encapsulation efficiency (EE) obtained for our studied system was 80%. The major components listed for citronella essential oil are citronellal, citronellol and β -pinene, which are easily solubilized in the Pluronic[®] nucleus, and this favored the encapsulation process. In Figure S4 (SI section), the UV-Vis absorbance used to calculate the EE is shown.

The *in vitro* study was conducted in order to understand the release mechanism of CEO from the obtained nanoparticulated system. Figure 6 shows the profile of CEO release from F127 nanoparticle covered with chitosan and sodium alginate for the two different media, analyzed over 24 h. In Figures S5a and S5b (SI section), the absorbance curves of CEO released in each studied medium were provided.

The release profile for both studied media showed an initial burst effect (up to 3 h), differing only in the

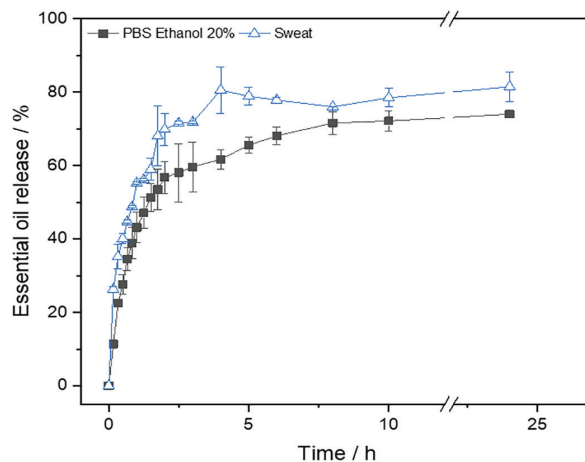


Figure 6. Experimental data and standard deviation bar for *in vitro* release profile for CEO-loaded nanoparticle in two different releasing media.

amount released. This first stage (burst region) of release can be explained by the fact that this amount of CEO is not entrapped in the polymeric system but adsorbed in the polymer surface³⁷ in which the release begins from contact with the dissolution medium.³⁸

The stabilization of release was reached at approximately 10 h in both studied media, with 74 and 81% of CEO released from nanoparticles for PBS 20% of ethanol and sweat medium, respectively. In agreement with the literature, pure F127 nanoparticles, or nanoparticles covered with chitosan only, do not satisfy the condition of essential oil release for a period of 24 h due to a very fast dissolution in both studied media. For this reason, we prepared nanoparticles with chitosan and sodium alginate coating, which remained stable for more than 24 h. The total amount released depends on diffusional equilibrium for each medium and the kinetic constant, which is shown in the next section.

Release kinetics for CEO from nanoparticle in dissolution media

Mathematical models already studied in literature³⁹⁻⁴² were used in order to investigate the mass transport mechanism involved in kinetic release utilizing a supplementary solver in Microsoft Excel. The data were adjusted to Higuchi, Korsmeyer-Peppas, zero and first order kinetic models according to the following equations:

$$\frac{M_t}{M_\infty} = K_H \sqrt{t} \quad (\text{Higuchi equation}) \quad (6)$$

$$\frac{M_t}{M_\infty} = kt^n \quad (\text{Korsmeyer-Peppas equation}) \quad (7)$$

$$F(t) = kt \quad (\text{zero order equation}) \quad (8)$$

$$\ln \left[1 - \frac{M_t}{M_\infty} \right] = -kt \quad (\text{first order equation}) \quad (9)$$

M_t represents the absolute quantity of active compound released at time t ; M_∞ the total amount of active compound released at infinite time for all equations above; K_H corresponds to the Higuchi constant, which

represents the characteristics of formulation structure. In the Korsmeyer-Peppas equation, k is a kinetic constant that concerns the structural mechanism and geometrical characteristics of the nanoparticle. The release exponent n denotes the active compound release mechanism. Thus, if $n \leq 0.43$ means purely Fickian diffusion, $n = 0.85$ means Case II of mass transport, namely polymer matrix relaxing or releasing through erosion. Intermediate n values $0.43 < n < 0.85$ indicate anomalous kinetic transport, the combination of both mechanisms.³⁹

However, the data did not adjust for zero or for first order for either studied medium. The Higuchi model did not have a strong correlation with data from the PBS 20% ethanol medium, whose correlation coefficient (R^2) = 0.421. Table 1 shows the values of parameters for the Korsmeyer-Peppas model. The linear form of equation 9, plotting $\ln M_t / M_\infty$ against $\ln t$, yielded the adjustment, $R^2 = 0.977$ and the kinetic constant = 40.51 for PBS 20% ethanol medium and $R^2 = 0.995$ and the kinetic constant = 52.25 for simulated sweat medium. A higher kinetic constant value obtained from sweat medium explained the faster release observed in the release profile graphic (Figure 6), which can be attributed to the presence of lactic acid in the sweat composition, since chitosan is hydrolyzed in aqueous solutions of acids. The Korsmeyer-Peppas empirical model considers the release mechanism as a combination of both Fickian transport and the Case II of mass transport controlled by polymer chain relaxation.⁴³ Analyzing the exponent n for spherical samples shows how the CEO release occurs. In the present evaluation, $n = 0.33$ and 0.37 , respectively, for PBS and sweat media, confirming that in both studies the CEO mechanism release occurs by diffusion.

Conclusions

A chitosan-sodium alginate polyelectrolyte complex was obtained based on the method known as ionic gelation. The electrostatic interaction between the two polymers was confirmed by FTIR analysis. This complex was used to cover Pluronic® F127 nanoparticles loaded with citronella essential oil. According to DLS measurements, the covering process increased the R_H size by about 30 nm. The complex was also important in stabilizing the nanoparticles,

Table 1. Kinetic parameters for *in vitro* CEO release in PBS and sweat medium

Model	PBS 20% ethanol			Sweat		
	R^2	k	n	R^2	k	n
Korsmeyer-Peppas	0.977	40.51	0.33	0.995	52.25	0.37

R^2 : correlation coefficient; k : kinetic constant; n : diffusional exponent.

and it is an interesting carrier system for hydrophobic compounds like citronella essential oil, which showed high encapsulation efficiency (80%) and was efficiently released in PBS/ethanol (70%) and sweat media (80%) for 24 h. These characteristics, associated with the nanoparticle stability in terms of size and zeta potential, allow a wide range of applications of this system.

Supplementary Information

Supplementary information is available free of charge at <http://jbcs.sbcq.org.br> as PDF file.

Acknowledgments

The present work was accomplished with the financial support of CAPES (Code 001). The authors are also grateful to LCME-UFSC for the microscopy images.

References

- Edris, A. E.; *Phytother. Res.* **2007**, *21*, 308.
- Sarkic, A.; Stappen, I.; *Cosmetics* **2018**, *5*, 11.
- Vieira, A. I.; Guerreiro, A.; Antunes, M. D.; Miguel, M. G.; Faleiro, M. L.; *Foods* **2019**, *8*, 57.
- Nelson, G.; *Int. J. Pharm.* **2002**, *242*, 55; Walenowska, J.; Foksowicz-Flaczyk, J.; *Int. Biodeterior. Biodegrad.* **2013**, *84*, 407.
- de Castro, J. A. M.; Monteiro, O. S.; Coutinho, D. F.; Rodrigues, A. A. C.; da Silva, J. K. R.; Maia, J. G. S.; *J. Braz. Chem. Soc.* **2019**, *30*, 930; Silva, C. F.; Moura, F. C.; *Braz. J. Chem. Eng.* **2011**, *28*, 343; Lee, M. Y.; *BioMed Res. Int.* **2018**, 6860271; Sendra, E.; *Foods* **2016**, *5*, 43.
- Li, W.-R.; Shi, Q.-S.; Ouyang, Y.-S.; Chen, Y.-B.; Duan, S.-S.; *Appl. Microbiol. Biotechnol.* **2013**, *97*, 7483; Nakahara, K.; Alzoreki, N. S.; Yoshihashi, T.; Nguyen, H. T. T.; Trakontivakorn, G.; *JARQ* **2003**, *37*, 249.
- Flores, F. C.; Ribeiro, R. F.; Ourique, A. F.; Rolim, C. M. B.; da Silva, C. B.; Pohlmann, A. R.; Beck, R. C. R.; Guterres, S. S.; *Quim. Nova* **2011**, *34*, 968.
- Ferrandiz, M.; López, A.; Franco, E.; Garcia-Garcia, D.; Fenollar, D.; Balart, R.; *Flavour Fragrance J.* **2017**, *32*, 184; Heydari, R.; Bavandi, S.; Javadian, S. R.; *Food Sci. Nutr.* **2015**, *3*, 188; Grande-Tovar, C. D.; Chaves-Lopez, C.; Serio, A.; Rossi, C.; Paparella, A.; *Trends Food Sci. Technol.* **2018**, *78*, 61; Hasheminejad, N.; Khodaiyan, F.; Safari, M.; *Food Chem.* **2019**, *275*, 113.
- Kaplan, D. L.; *Biopolymers from Renewable Sources*; Springer: New York, USA, 1998.
- Stender, E. G. P.; Khan, S.; Ipsen, R.; Madsen, R.; Madsen, F.; Haglluund, P.; Hachem, M. A.; Almdal, K.; Westh, P.; Svensson, B.; *Food Hydrocolloids* **2018**, *75*, 175.
- Kamburova, K.; Mitarova, K.; Radeva, T.; *Colloids Surf., A* **2017**, *519*, 199.
- Yang, J.; Han, S.; Zheng, H.; Dong, H.; Liu, J.; *Carbohydr. Polym.* **2015**, *123*, 56.
- Oliveira, S. P. L. F.; Bertan, L. C.; de Rensis, C. M. V. B.; Bilck, A. P.; Vianna, P. C. B.; *Polimeros* **2017**, *27*, 158.
- Oliveira, S. A.; Moura, C. L.; Cavalcante, I. M.; Lopes, A. A.; Leal, L. K. A. M.; Gramosa, N. V.; Ribeiro, M. E. N. P.; França, F. C. F.; Yeates, S. G.; Ricardo, N. M. P. S.; *J. Braz. Chem. Soc.* **2015**, *26*, 2195.
- Chat, O. A.; Nazir, N.; Bhat, P. A.; Hassan, P. A.; Aswal, V. K.; Dar, A. A.; *Langmuir* **2018**, *34*, 1010.
- Natrajan, D.; Srinivasan, S.; Sundar, K.; Ravindran, A.; *J. Food Drug Anal.* **2015**, *23*, 560.
- Kulthong, K.; Srisung, S.; Boonpavanitchakul, K.; Kangwansupamonkon, W.; Maniratanachote, R.; *Part. Fibre Toxicol.* **2010**, *7*, 8.
- Alves-Silva, J. M.; Zuzarte, M.; Gonçalves, M. J.; Cavaleiro, C.; Cruz, M. T.; Cardoso, S. M.; Salgueiro, L.; *Evidence-Based Complementary Altern. Med.* **2016**, *2016*, 9045196.
- El-Kholany, E. A.; *Int. J. Microbiol. Biotechnol.* **2016**, *1*, 49.
- Specos, M. M. M.; *Trans. R. Soc. Trop. Med. Hyg.* **2010**, *104*, 653.
- ALV 7004 V. 3.0, *Correlator Software Interfaced to the Multicorrelator Goniometer Model ALV-LSE 5004*; ALV, Germany, 2014.
- Avadi, M. R.; Sadeghi, A. M. M.; Mohammadpour, N.; Abedin, S.; Atyabi, F.; Dinarvand, R.; Rafiee-Teharani, M.; *Nanomed. Nanotechnol.* **2010**, *6*, 58.
- Ashraf, U.; Chat, O. A.; Maswal, M.; Jabeen, S.; Dar, A. A.; *RSC Adv.* **2015**, *5*, 83608.
- Basak, R.; Bandyopadhyay, R.; *Langmuir* **2013**, *29*, 4350.
- Pepic, I.; Filipovic-Grcic, J.; Jallenjak, I.; *Colloids Surf., A* **2008**, *327*, 95.
- Branca, C.; Khouzami, K.; Wanderlingh, U.; D'Angelo, G.; *J. Colloid Interface Sci.* **2018**, *517*, 221.
- Shu, S.; Zhang, X.; Teng, D.; Wang, Z.; Li, C.; *Carbohydr. Res.* **2009**, *344*, 1197.
- Wu, C.; Wang, L.; Hu, Y.; Chen, S.; Liu, D.; Ye, X.; *RSC Adv.* **2016**, *6*, 20892.
- Furtado, G. T. F. S.; Fideles, T. B.; Cruz, R. C. A. L.; Souza, J. W. L.; Barbero, M. A. R.; Fook, M. V. L.; *Mater. Res.* **2018**, *21*, e20180101.
- Shao, Y.; Wu, C.; Wu, T.; Li, Y.; Chen, S.; Yuan, C.; Hu, Y.; *Carbohydr. Polym.* **2018**, *193*, 144.
- Barradas, T. N.; Senna, J. P.; Cardoso, S. A.; Nicoli, S.; Padula, C.; Santi, P.; Rossi, F.; Silva, K. G. H.; Mansur, C. R. E.; *Eur. J. Pharm. Biopharm.* **2017**, *116*, 38.
- Tagliari, M. P.; Granada, A.; Kuminek, G.; Stulzer, H. K.; Silva, M. A. S.; *Quim. Nova* **2012**, *35*, 1228.

33. Guerra-Rosas, M. I.; Morales-Castro, J.; Ochoa-Martinez, L. A.; Silva-Trujillo, L.; Martín-Belloso, O.; *Food Hydrocolloids* **2016**, *52*, 438.
34. Brugnerotto, J.; Lizardi, J.; Goycoolea, F. M.; Arguelles-Monal, W.; Desbrieres, J.; Rinaudo, M.; *Polymer* **2001**, *42*, 3569.
35. Filippov, M. P.; Kohn, R.; *Chem. Zvesti* **1974**, *28*, 817.
36. Zhao, Y.; Shen, W.; Chen, Z.; Wu, T.; *Carbohydr. Polym.* **2016**, *148*, 45.
37. Kumari, A.; Yadav, S. K.; Yadav, S. C.; *Colloids Surf., B* **2010**, *75*, 1.
38. Huang, X.; Brazel, C. S.; *J. Controlled Release* **2001**, *73*, 121.
39. Ritger, P. L.; Peppas, N. A.; *J. Controlled Release* **1987**, *5*, 23.
40. Ritger, P. L.; Peppas, N. A.; *J. Controlled Release* **1987**, *5*, 37.
41. Peppas, N. A.; Sahlin, J. J.; *Int. J. Pharm.* **1989**, *57*, 169.
42. Peppas, N. A.; Siepmann, J.; *Int. J. Pharm.* **2011**, *418*, 6.
43. Khazaei, A.; Saednia, S.; Saien, J.; Kazem-Rostami, M.; Sadeghpour, M.; Borazjani, M. K.; Abbasi, F.; *J. Braz. Chem. Soc.* **2013**, *24*, 1109.

Submitted: May 20, 2019

Published online: October 14, 2019

